Research Article

Miriam Grava, Sally Helmy, Mario Gimona, Pietro Parisse, Loredana Casalis, Paola Brocca*, Valeria Rondelli*

Calorimetry of extracellular vesicles fusion to single phospholipid membrane

https://doi.org/10.1515/bmc-2022-0011
received January 31, 2022; accepted March 1, 2022

Abstract: Extracellular vesicles (EVs)-mediated communication relies not only on the delivery of complex molecular cargoes as lipids, proteins, genetic material, and metabolites to their target cells but also on the modification of the cell surface local properties induced by the eventual fusion of EVs' membranes with the cells' plasma membrane. Here we applied scanning calorimetry to study the phase transition of single phospholipid (DMPC) monolamellar vesicles, investigating the thermodynamical effects caused by the fusion of doping amounts of mesenchymal stem cells-derived EVs. Specifically, we studied EVs-induced consequences on the lipids distributed in the differently curved membrane leaflets, having different density and order. The effect of EV components was found to be not homogeneous in the two leaflets, the inner (more disordered one) being mainly affected. Fusion resulted in phospholipid membrane flattening associated with lipid ordering, while the transition cooperativity, linked to membrane domains' coexistence during the transition process, was decreased. Our results open new horizons for the investigation of the peculiar effects of EVs of different origins on target cell membrane properties and functionality.

* **Corresponding author: Paola Brocca,** Department of Medical Biotechnology and Translational Medicine, Università Degli Studi di Milano, Milano, Italy, e-mail: paola.brocca@unimi.it
* **Corresponding author: Valeria Rondelli,** Department of Medical Biotechnology and Translational Medicine, Università Degli Studi di Milano, Milano, Italy, e-mail: valeria.rondelli@unimi.it
Miriam Grava: Institute for Condensed Matter Physics, Department of Physics, Technische Universität Darmstadt, Darmstadt, Germany
Sally Helmy: Department of Medical Biotechnology and Translational Medicine, Università Degli Studi di Milano, Milano, Italy; Biophysics Group, Physics Department, Faculty of Science, Ain Shams University, Cairo, Egypt
Mario Gimona: GMP Unit, Spinal Cord Injury and Tissue Regeneration Center Salzburg, Paracelsus Medical University (PMU), Salzburg, Austria; Research Program "Nanovesicular Therapies", Paracelsus Medical University, Salzburg, Austria
Pietro Parisse: Istituto Officina dei Materiali, Department of Physical sciences and technologies of matter, Italian National Research Council, Trieste, Italy
Loredana Casalis: NanoInnovation Lab, Elettra Sincrotrone Trieste, Trieste, Italy

Introduction

Extracellular vesicles (EVs) are produced by cells and released in the intercellular medium in order to deliver their cargo molecules as proteins and genetic material between cells and through the organs and tissues of the body. The number of EVs released and internalized depends on the cell line of the originating cell and on the target cell, their physiological state, and the surrounding medium [1]. In the past years they received increasing attention for their fundamental role in intercellular communication. In fact, they contain specific signatures from the originating cells, they can strongly influence the fate of the recipient cells, and they have a crucial role in the diffusion of pathologies as cancer and neurodegenerative disorders [2,3]. Hence, EVs have been proposed as biomarkers for several diseases [4].

In this landscape, our aim is to investigate the fusion mechanisms of EVs of different origins with model membranes and to understand the effects of EV components on the thermotropic properties of the target model membranes, using EVs-doped simple systems. To our scope, we performed calorimetry on single phospholipid large unilamellar vesicles (LUVs) mixed with EVs in different proportions.

In a previous analysis [5] we proposed a multi-technique/multiscale investigation on EVs from mesenchymal stem cells in interaction with model membrane systems of variable complex compositions and unveiled a strong interaction of EVs with the model membranes and preferentially with the borders of protruding phase domains. We are going forward in this direction to analyze the impact of the same EVs on the thermotropic behavior of phospholipids, the main membrane components.

By applying differential scanning calorimetry (DSC) on EVs-doped phospholipid LUVs, we see the effect brought by the components of EVs to the target

membrane lipids in terms of fluidity and cooperativity of the melting phase transition. The structural changes occurring at phospholipid melting transition are similar to the fluctuations of fluid membranes, thus their investigation is of importance in view of understanding the mutual relation between membrane dynamics and embedded proteins. Cell functionality is associated with membranes of highly dynamic structures, where protein sorting may be driven by local phase fluctuations involving thickening and thinning of the membrane. Indeed, melting phase transition of phospholipids show characters typical of a first order phase transition; nevertheless, it also exhibits several anomalies of the system more typical of second order transition, with pseudocritical behavior of physico-chemical parameters such as interlayer distance in multilamellar vesicles, membrane permeability, and lateral compressibility [6–9]. It is of interest to underline that these anomalies have been associated with critical out of plane fluctuations of the membranes, coupled with critical lengthening of the decay of short range interactions, and with softening of the bilayer when approaching the transition [10].

In the present work, we study the first order aspects of the melting/gelling transition in LUVs, specifically, we exploit the peculiarity of 1,2-Dimyristoyl-sn-glycero-3-phosphocholine (DMPC) LUVs, extruded trough 80 nm sized pore filters, to show 2 distinct contributions to the enthalpic peak associated with the inner and outer membrane leaflets [11–14]. Indeed, the packing of the lipids in the two leaflets is asymmetrically affected by the curvature imposed by extrusion. We can thus distinguish asymmetric effect of the EV components on the lipids belonging to the two layers.

Materials and methods

Isolation of human mesenchymal stromal cell-derived EVs

Vesicles have been isolated and purified from umbilical cord mesenchymal stem cells by filtration and centrifugation with the protocol described in ref. [5] and quantified to be 2×10^9 EVs in 100 µL by nanoparticle tracking analysis (NTA).

Lipids for model membranes

DMPC was purchased from Avanti Polar Lipids (Alabama) and used without any further purification.

Lipid LUVs preparation for model membranes fabrication

Model lipid-based membranes were prepared with a standard procedure explained in ref. [15] by thin film deposition, hydration, and extrusion.

Lipid molecules were dissolved in chloroform, an appropriate organic solvent. Lipid solutions were then deposited on round bottom boiling flasks. After the organic solvent evaporated under a gentle stream of nitrogen, samples were placed under vacuum to completely remove solvent residues and re-suspended in 60 mM ringer buffer, a solution that well simulates body fluids and in which EVs are suspended. Freeze-thawing method was applied to reduce the number of overlapping bilayers. It consists in treating the samples with repetitive cycles ($n = 5$) of freezing in liquid nitrogen and thawing in warm water. Then, samples were extruded 51 times through two polycarbonate membrane filters with 80 nm sized pores using a commercial extruder (Avanti Polar Lipids), to form LUVs at 2% concentration.

DSC

We performed calorimetry measurements on samples composed by DMPC LUVs in interaction with different quantities of mesenchymal stem cells-derived EVs. Specifically, EVs were added to 250 µL of LUV solution in number (quantified by NTA) being of 5×10^8, 10×10^8, and 20×10^8. We underline that NTA is sensitive to aggregates bigger than ~50 nm, while our previous investigation [5] indicated that the used EVs sample also contains important amount of smaller objects.

DSC measurements were carried out by means of non-commercial Double Differential Scanning Calorimeter (MASC), built at the laboratories of the Istituto per i Processi Chimico-Fisici (IPCF) at the CNR of Pisa, Italy [16], that contains two identical cells, one with the sample in solution and the other with a reference material that does not present phase transitions in the temperature range to be explored, both placed in glass capillaries. Varying the temperature over time in a controlled manner and measuring the difference between the power supplied to the two cells, it is possible to measure the variation in specific heat. The accessible temperature range is from −20 to 200°C with a sensitivity of 0.002°C, and power sensitivity is ±30 µW. The samples were submitted to temperature cycles in the range: $10°C < T < 45°C$ at a scan rate of 1°C/3 min, both in heating and cooling modes. Before the beginning of each measurement, an

isotherm was imposed for 1 h at 45°C, to let the sample incubate and for the sample and instrument to reach the thermal equilibrium. Before and after each cycle, an isotherm was imposed for 1,800 s at the starting of scanning temperatures, that is 10°C before heating and 45°C before cooling.

Dynamic light scattering (DLS)

DLS measurements were performed at 90° with a non-commercial apparatus [17] with $\lambda = 532$ nm Nd:YAG laser source at $T = 20$°C.

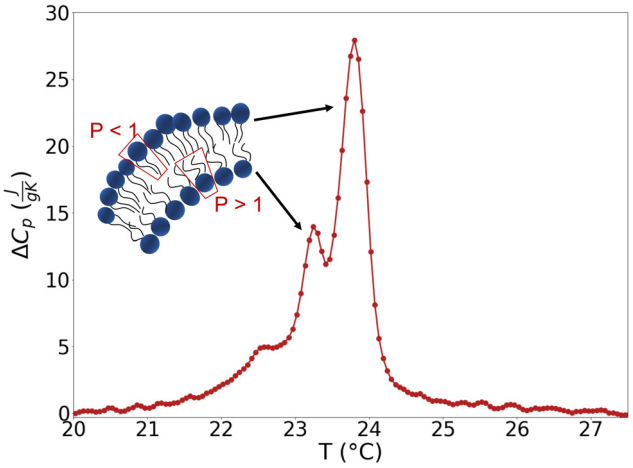

Figure 1: Trend of the specific heat ΔC_p at varying temperatures obtained by DSC measurements on DMPC LUVs in ringer buffer. Scan rate 3°C/min, cooling mode.

Results

The geometric properties of amphiphilic aggregates depend on three parameters concerning the hydrocarbon chains of the lipid core: the volume V occupied by the hydrophobic part of each monomer ($V_{\text{hydrophobic}}$), the chain length (l_c), and the area (a_0) covered by the hydrophilic head.

The packing parameter is defined as:

$$P = \frac{V_{\text{hydrophobic}}}{a_0 l_c}.$$

In planar membranes, P is equal to 1, while in curved systems, P can assume values higher/lower than 1 depending on the curvature of the layer which can either be concave or convex. In DMPC bilayer forced to close in LUVs, the lipid chains populating the inner layer have a higher specific volume (less ordered state) than the ones in the outer layer (more ordered state), as a consequence of the molecules-imposed geometry. The asymmetric arrangement in DMPC LUVs was recently quantified by modeling of the gel state [18].

The thermodynamic behavior in the melting of the same lipid can diverge depending on its starting packing in gel phase. This peculiarity is exploited in the present investigation.

DSC measurements were performed on LUVs of DMPC at the concentration of 60 mM in ringer buffer, before and after interaction with incremental doses of EVs. The thermotropic behavior of lipid LUVs may depend on the used buffer. Figure 1 reports the measured specific heat capacity $\Delta C_p(T)$ for our system, showing similar features to DMPC LUVs in water, with measured transition enthalpy $\Delta H_{\text{cal}} = 25.1 \pm 0.5$ J/g, in agreement with literature [19].

The complexity of the enthalpic peak departs from the single steep peak observed for melting transition of multilamellar phospholipid systems [19,20] highlighting a broadening of the first order aspects of the transition in LUVs. The two main enthalpic peaks detected are centered at $T = 23.24$°C and $T = 23.79$°C. The interpretation of the two contributions is not trivial, but they are known to occur in vesicles of short chain phospholipids (up to DMPC) for reasons of their degree curvature [12]. The interpretation proposed in the past for LUVs extruded on 100 or 200 nm pore sized filters that associated the two calorimetric peaks with monolamellar and multilamellar contributions [11] can be excluded after extrusion on 80 nm sized pore membrane by SANS evidence [21]. Previous coupled DSC and densitometry investigation [12] proposed lateral segregation of differently dense and curved domains arising in the fluctuating membrane during the stepwise gel–fluid transition [22]; other authors univocally interpreted [13,14] the two peaks as related to the inner and outer layers of the phospholipid membrane having different density/packing geometries. As, in membrane systems, the two coexisting phases during melting/gelling transition occur in a 'mosaic-like model' domains [23,24] of the incoming phase growing in the original phase, here, for short chain highly curved bilayer, a decoupling of the convex and concave monolayers transition must be considered due to the fact that those facing domains have different densities in gel phase [18].

The peak separation will therefore be associated, in the following, with different starting packing modes of the lipids in concave/inner and convex/outer monolayer domains. In particular, the lower temperature peak will

Table 1: Thermodynamic parameters obtained for the two LUVs leaflets at varying EVs content

	DMPC		DMPC + EVs		DMPC + EVs × 2		DMPC + EVs × 4	
	Inner	Outer	Inner	Outer	Inner	Outer	Inner	Outer
$T_{melting}$ (±0.01°C)	23.24	23.78	23.25	23.79	23.26	23.80	23.26	23.81
ΔC_p maximum (±0.01 J/g K)	9.59	27.29	9.55	26.47	9.79	26.13	10.57	26.13
ΔH_{VH} (J/g)	5,743	5,259	5,442	5,261	5,076	5,261	5,075	5,262
ΔH_{Cal} (±0.2 J/g)	4.9	15.8	5.2	15.3	5.8	15.1	6.2	15.1
$\frac{\Delta H_{VH}}{\Delta H_{Cal}}$ cooperative units	1,160	333	1,040	344	875	348	811	348
Area cooperative unit (nm^2)	696	186	624	193	525	195	487	195

be related to the inner layer and the higher temperature peak to the outer layer of the phospholipid membrane of LUVs.

DMPC + different EV concentrations

Before performing DSC investigation on EVs–LUVs mixed systems, the effect of fusion on the LUVs size has been investigated by DLS. EVs–LUVs mixing occurred with 1 h incubation at 45°C. The hydrodynamic radius, found to be 44 nm (1% polydispersity and 1.5% variance) for DMPC LUVs at 20°C, increases up to 58 nm (1% polydispersity and 1.5% variance) after the interaction with doping EVs, whose size was found to be 120 ± 50 nm [5].

Mixing DMPC LUVs with doping amounts of EVs, we observe a modification of the shape of $\Delta C_p(T)$. More specifically, the effects are not the same in the two peaks, being more evident on the lower temperature peak (T_m = 23.24°C) associated with the concave inner layer (Table 1).

After EVs mixing (Figure 2), the melting temperature slightly increases for both the inner and the outer leaflets, with a stronger effect on the inner one. The total transition enthalpy is increased by 2%. These findings suggest that in the mixed system, the DMPC phospholipids assume a more ordered configuration in the gel phase. This feature is in agreement with the increase in hydrodynamic radius as measured by DLS for the LUVs.

It is important to compare the behavior of the systems during cooling and heating. Figure 1S of SI reports the heating scans subsequent to the cooling ones found in Figure 1. Figure 2S of the SI shows that the splitting of the two peaks of the melting transition (ΔT = 0.41°C) is smaller than that observed upon gelling (ΔT = 0.55°C). Indeed, the gelling process requires the nucleation of the new phase to start, oppositely to the melting one. The different splitting demonstrates that the process associated with the low temperature peak of concave/inner layer involves lipids less prone to nucleate the ordered phase with respect to convex/outer lipids. This feature linked to observed asymmetric influence of EVs on the

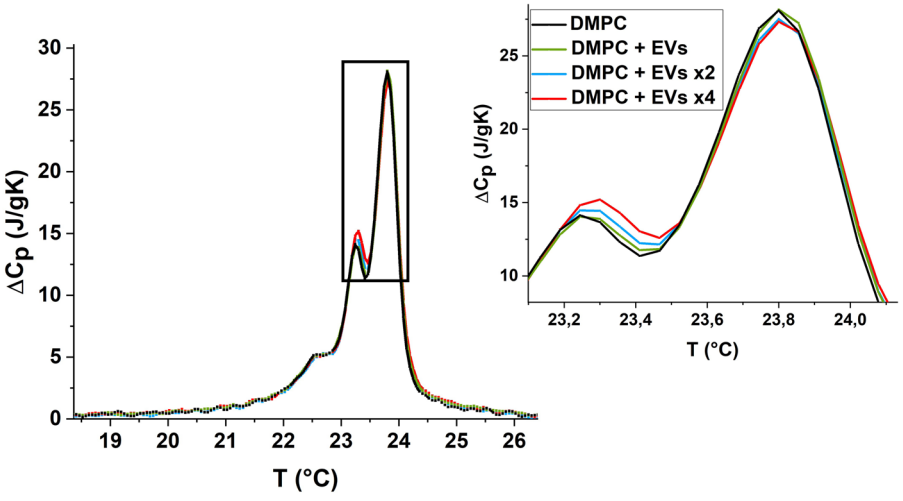

Figure 2: Trend of $\Delta C_p(T)$ of DMPC LUVs after addition of increasing amounts of EVs.

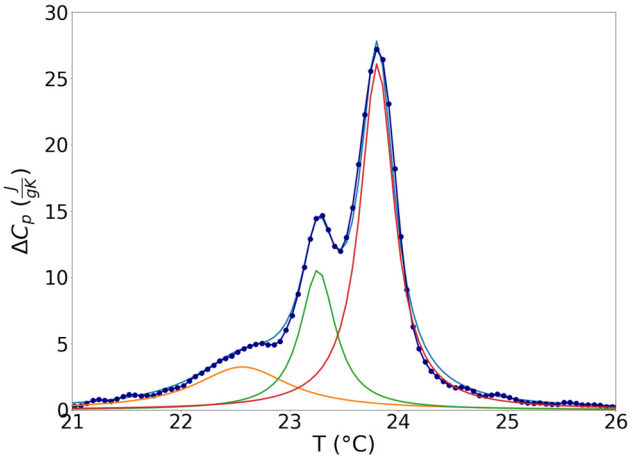

Figure 3: Fit of $\Delta C_p(T)$ trend for DMPC LUVs after the last EVs addition to the system.

two enthalpic peaks suggests that the physical processes under the two events are well distinct, and that EVs effect depends on the physical properties of the lipid domains where they interact.

Thus, in order to deepen the role played by EVs in interaction with lipids in different ordered states, we followed the working hypothesis to analyze separately the two enthalpic contributions (Figure 3). Peak analysis was developed on the cooling thermographs where peaks are more separated, by modeling the trend of $\Delta C_p(T)$ (that is $C_p(T)$ from which a straight oblique baseline was subtracted to bring its value to zero before and after the enthalpic peak) with a linear combination of three Lorentzians. Indeed, beside the two main enthalpic peaks, a third broad and less intense one can be distinguished in the

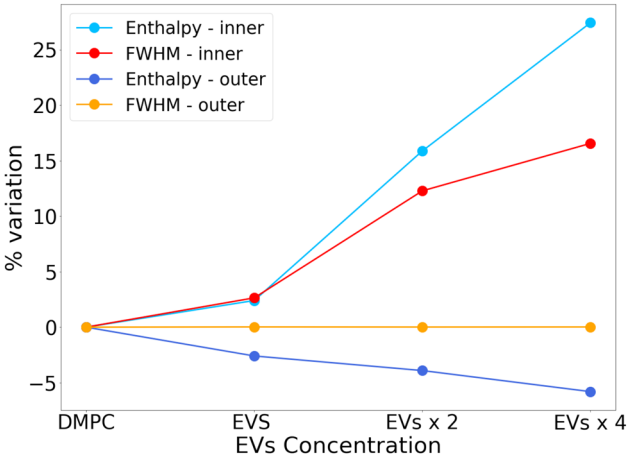

Figure 4: Trend of the percentage change in thermodynamic parameters at varying EVs addition to DMPC LUVs for the two distinguished LUVs leaflets.

region of lower temperature in the main melting transition centered around $T = 22.57$°C. The attribution of this peak is not straightforward, and our interpretation is that it may be originated from structures other than LUVs present in the sample, or by disordered defects in the LUVs under study. Nonetheless, EV components do not affect this peak, which can be modeled as conserved during the analysis.

Figure 4 reports the trend of the percentage change in thermodynamic parameters for increasing amount of incubated EVs distinguishing the two opposite curved layers with different degrees of order. The transition enthalpy (Table 1) of the peak relative to the outer layer decreases by 5% and, consistently, a slight decrease in ΔC_p max is observed. The outer layer, which in pure DMPC LUVs sample is in a more ordered state, is brought to a more disordered state as the amount of EVs inserted into the sample increases. On the opposite, the inner layer transition enthalpy increases by 27% after EVs mixing, supporting the evidence of an ordering effect on the more disordered target lipids.

Therefore, lipids, sterols, and proteins brought by EVs, once inserted into the DMPC model membrane, reduce the disparity between the two layers. This effect is more pronounced on the lipids belonging to the inner layer of the membrane, which before the interaction were in a more disordered state.

Finite systems have a phase transition with a trend of specific heat described by an expanded function if compared to ideal systems with first order transition where C_p at varying temperatures is described by a Dirac delta. For lipid bilayers, the reported broadening of the enthalpic peak is associated with a finite, low, cooperativity of the transition. By analyzing the shape of $\Delta C_p(T)$, it is then possible to obtain information on the cooperativity of the transition.

Assuming to consider the transition of the inner and outer lipids as decoupled, a model of two states transition between the *gel* phase and the *fluid* phase is applied following the Van't Hoff's relation [25,26], reported here in terms of the fractional amount of transited lipids, f, vs temperature, allowing us to estimate the cooperative units (equation [1]). The fit of the integral of $\Delta C_p(T)$ is performed for each peak and

$$f = 1 - \frac{1}{1 + \exp\left(-\frac{\Delta H_{VH}}{RT}\left(1 - \frac{T}{T_m}\right)\right)}, \qquad (1)$$

where the Van't Hoff enthalpy ΔH_{VH} is evaluated together with T_m (temperature at which 50% lipids are found in the growing phase). The number of cooperative units in the transition was obtained as the ratio between the

derived Van't Hoff enthalpy and the measured calorimetric enthalpy.

The area-per-lipid (APL) for DMPC was obtained by molecular dynamics simulations on giant unilamellar vesicles (GUVs) [18]. APL was calculated considering the thickness of the membrane as the difference between the radius of the outer and inner layers, having defined the APL separately for the inner and outer layers of the membrane and for the vesicle considered as a whole. The area of the cooperative unit was calculated as the product of APL and the number of cooperative units and is reported in Table 1.

The inner layer transition of the empty DMPC LUVs is found to be very cooperative. The number of cooperative units (n_{in}) in the inner layer, found to be 1,160, was then decreased as EVs were added to the system, while for the outer layer, the cooperative unit (n_{out}) was found to be 333, almost conserved as EVs interact with LUVs (Table 1). The cooperative units' value n_{in} is very high if compared to what is found for the whole transition, evaluated to be 187 for DMPC and decreasing to 176 after EVs addition. However, our results compare favorably with recent measurements on DMPC LUVs studied by adiabatic scanning calorimetry and quartz crystal microbalance with dissipation [27] where the inner and outer events had been decoupled. The cooperative unit corresponds to about 1% and about 0.4% of the total lipids in a layer for the inner and outer lipids, respectively. The effect of EVs is more evident on the inner lipids, originally less ordered before the interaction with the EVs. Indeed, a decreased cooperativity indicates an increased membrane parcellation of the coexisting fluid and gel domains during the transition [26] that is induced by the inclusion of EV components in the membranes. It is possible to give a rough quantitative estimation of the lengthening of the border of the cooperative domains implied by the decrease in units after EVs fusion (by considering a circular geometry for the arrangement of lipids belonging to a unit). A 5% increase in edges with the first addition, a 15% with the second addition, and 20% with the third addition can be evaluated. Atomic force microscopy (AFM) in dipalmitoylphosphatidylcholine phospholipid/Sphingomyelin/cholesterol membrane, where liquid-liquid phase separation occurs at room temperature, showed that the same EVs preferentially fused at the phase domain borders and, remarkably, EVs fusion induced an increase in the length of the domain borders. This phenomenon was ascribed to a decrease in the line tension produced by the EVs that eventually partially recover the thickness mismatch between the two liquid phases. In our study, we hypothesize that an analogous landscape happens to occur inside the melting transition, where DSC is sensitive to the thermotropic counterpart of the same rim energy decrease induced by EV components that broaden the transition (decreased cooperativity). It is worthwhile to recall that although only dopant amount of EVs is used, by making them act along a line border, a major effect is induced.

Summing up, we recall that the broadening of the peaks shows up together with T_m and ΔH variation. T_m and ΔH increase in the concave/inner lipids population indicates that EVs impose a higher order/rigidity to the originally more disordered/less dense lipids on the local scale. This is consistent with a flattening of the membrane domains, maybe helped by the domains parcellation disclosed by peak broadening. For the convex/outer lipids T_m, increases as well, while ΔH decreases. A partial redistribution of lipids between the two layers may account for the apparent ΔH transfer among the two peaks, accompanying flattening. The overall increase in T_m and ΔH denotes an ordering effect on target lipids acted by the doping EVs, also in agreement with the increased size of the overall vesicular aggregates. Such behavior possibly implies a decrease in lipids'/domains' lateral mobility within the membrane.

Conclusion

DSC is still poorly used in the field of EV investigation and in the study of their internalization mechanisms, as model membranes are still poorly exploited in this expanding field, presenting plenty of unknown aspects. We applied DSC and model membrane systems to achieve new information on EVs' internalization effects on target membrane phospholipids, starting from EVs well characterized by us in terms of chemico-physical properties and internalization mechanisms [5].

We exploited the peculiarity of DMPC LUVs to show two distinct contributions to the enthalpic peak of the main melting transition associated with the oppositely curved inner and outer membrane leaflets. We can distinguish a strong effect on the lipids belonging to the inner concave layer having lower density in the gel phase: as the amount of EVs interacting with model LUVs increases, there is a roughly 30% increase in relative transition enthalpy. The overall outcome is an augmented melting temperature and excess enthalpy after EVs doping, consistent with an overall flattening of the membrane associated with lipids ordering, also in agreement with the observed increased size of the LUVs. Such behavior possibly implies, a decrease in lipids'/domains' lateral mobility within the membrane. Moreover, the

cooperativity of the transition was observed to decrease after EVs fusion. This last finding strengthens previous observation [5] by AFM on liquid-liquid phase separated complex membranes, where EVs have been observed to fuse decreasing the line tension between liquid ordered and fluid domains, possibly partially recovering the thickness mismatch between the two phases. In our study, the thermotropic counterpart of the same effect is seen on the melted/unmelted domains inside the transition as suggested by the broadening of the enthalpic peaks.

Local fluctuations, occurring at membrane melting transition, can drive the dynamical response of EV components in target bilayer of importance if considered at the cell scale, where such dynamics impact functionality.

The finding here presented may be related to the peculiarities of the EVs used for the study, and a different situation may show up if EVs of different origin are mixed with the DMPC LUVs. Thus, our approach can be relevant in increasing the knowledge on specific EVs fusion consequences on target cells. In fact, not only cargo delivery may have important roles in EVs-mediated communication, but also EV molecules' effects on target cell membrane properties. In natural membranes, those properties have fundamental roles for the selective lateral segregation of specific molecules, and in particular proteins [28], and this is of pivotal importance for the whole cell functionality. In this perspective, our findings open new horizon for the investigation of the role of EVs on target cells surface organization and functionality.

Acknowledgements: Authors acknowledge the "Medical Biotechnology and Translational Medicine Department" of the "Università degli Studi di Milano", grant numbers "PSR2018" and "PSR2020" to V.R. and to P.B.

Funding information: Gimona gratefully acknowledges financial support through the projects "Exothera IT-AT 1036" (European Regional Development Fund and Interreg V-A Italia – Austria 2014–2020), "ExtraNeu" (Land Salzburg/WISS 2025), P1812596 "EV-TT" (Land Salzburg/IWB/EFRE), 20102-F1900731-KZP "EV-TT – Bpro" (Land Salzburg/WISS 2025) and "Medical Biotechnology and Translational Medicine Department" of the "Università degli Studi di Milano", grant numbers PSR2018 and PSR2020 to V.R. and to P.B. S. Helmy is founded by a full scholarship (mission 2019/2020) from the Ministry of Higher Education in Egypt. The current research work is not founded by the mentioned ministry of Egypt.

Conflict of interest: Authors state no conflict of interest.

Data availability statement: The datasets generated during and/or analyzed during the current study are available from the corresponding author on reasonable request.

References

[1] Caponnetto F, Manini I, Skrap M, Palmai-Pallag T, Di Loreto C, Beltrami AP, et al. Size-dependent cellular uptake of exosomes. Nanomed Nanotechnol Biol Med. 2017 Apr 1;13(3):1011–20.

[2] Doyle LM, Wang MZ. Overview of extracellular vesicles, their origin, composition, purpose, and methods for exosome isolation and analysis. Cells. 2019 Jul;8(7):727.

[3] Paolini L, Zendrini A, Radeghieri A. Biophysical properties of extracellular vesicles in diagnostics. Biomarkers Med. 2018 Apr;12(4):383–91.

[4] Murphy DE, de Jong OG, Brouwer M, Wood MJ, Lavieu G, Schiffelers RM, et al. Extracellular vesicle-based therapeutics: natural versus engineered targeting and trafficking. Exp Mol Med. 2019 Mar;51(3):1–2.

[5] Perissinotto F, Rondelli V, Senigagliesi B, Brocca P, Almásy L, Bottyán L, et al. Structural insights into fusion mechanisms of small extracellular vesicles with model plasma membranes. Nanoscale. 2021;13(10):5224–33.

[6] Zhang R, Sun W, Tristram-Nagle S, Headrick RL, Suter RM, Nagle JF. Critical fluctuations in membranes. Phys Rev Lett. 1995;74:2832.

[7] Albrecht O, Gruler H, Sackmann E. Polymorphism of phospholipid monolayers. J Phys. 1978;39:301–13.

[8] Hønger T, Mortensen K, Ipsen JH, Lemmich J, Bauer R, Mouritsen OG. Anomalous swelling of multilamellar lipid bilayers in the transition region by renormalization of curvature elasticity. Phys Rev Lett. 1994;72:3911.

[9] Brocca P, Cantù L, Corti M, Del Favero E, Motta S, Nodari MC. DC(13)PC bilayers from anomalous swelling to main transition: an X-ray scattering investigation. J Colloid Interface Sci. 2007;312(1):34–41.

[10] Kuklin A, Zabelskii D, Gordeliy I, Teixeira J, Brûlet A, Chupin V, et al. On the origin of the anomalous behavior of lipid membrane properties in the vicinity of the chain-melting phase transition. Sci Rep. 2020;10:5749.

[11] Drazenovic J, Wang H, Roth K, Zhang J, Ahmed S, Chen Y, et al. Effect of lamellarity and size on calorimetric phase transitions in single component phosphatidylcholine vesicles. Biochim Biophys Acta (BBA)-Biomembranes. 2015 Feb 1;1848(2):532–43.

[12] Brocca P, Cantu L, Corti M, Del Favero E, Motta S, Nodari MC. Curved single-bilayers in the region of the anomalous swelling: Effect of curvature and chain length. Colloids Surf A: Physicochem Eng Asp. 2006;291(1–3):63–8.

[13] Pham Quoc D. Effects of oxidized phospholipids and heavy water on the structure of phospholipid bilayer membranes. [Master thesis]; 2011.

[14] Doktorova M, Heberle FA, Marquardt D, Rusinova R, Sanford RL, Peyear TA, et al. Gramicidin increases lipid flip-

flop in symmetric and asymmetric lipid vesicles. Biophys J. 2019 Mar 5;116(5):860–73.
[15] Rondelli V, Brocca P, Tranquilli N, Fragneto G, Del Favero E, Cantù L. Building a biomimetic membrane for neutron reflectivity investigation: complexity, asymmetry and contrast. Biophys Chem. 2017 Oct 1;229:135–41.
[16] Salvetti G, Cardelli C, Ferrari C, Tombari E. A modulated adiabatic scanning calorimeter (MASC). Thermochim acta. 2000 Dec 1;364(1–2):11–22.
[17] Lago P, Rovati L, Cantù L, Corti M. A quasielastic light scattering detector for chromatographic analysis. Rev Sci Instrum. 1993 Jul;64(7):1797–802.
[18] Drabik D, Chodaczek G, Kraszewski S, Langner M. Mechanical properties determination of DMPC, DPPC, DSPC, and HSPC solid-ordered bilayers. Langmuir. 2020 Mar 16;36(14):3826–35.
[19] Koynova R, Caffrey M. Phases and phase transitions of the phosphatidylcholines. Biochim Biophys Acta (BBA) - Rev Biomembranes. 1998;1376(1):91–145.
[20] Ebel H, Grabitz P, Heimburg T. Enthalpy and volume changes in lipid membranes. I. The proportionality of heat and volume changes in the lipid melting transition and its implication for the elastic constants. J Phys Chem B. 2001;105:7353–60.
[21] Perissinotto F, Rondelli V, Parisse P, Tormena N, Zunino A, Almásy L, et al. GM1 ganglioside role in the interaction of alpha-synuclein with lipid membranes: morphology and structure. Biophys Chem. 2019 Dec 1;255:106272.
[22] Ipsen JH, Jørgensen K, Mouritsen OG. Density fluctuations in saturated phospholipid bilayers increase as the acyl-chain length decreases. Biophys J. 1990 Nov 1;58(5):1099–107.
[23] Mouritsen OG, Zuckermann MJ. Softening of lipid bilayers. Eur Biophys J. 1985 Jun 1;12(2):75–86.
[24] Alessandrini A, Facci P. Phase transitions in supported lipid bilayers studied by AFM. Soft Matter. 2014;10(37):7145–64.
[25] Sturtevant JM. Biochemical applications of differential scanning calorimetry. Annu Rev Phys Chem. 1987;38:466–76.
[26] Raudino A, Sarpietro MG, Pannuzzo M. The thermodynamics of simple biomembrane mimetic systems. J Pharm Bioallied Sci. 2011;3(1):15–38. doi: 10.4103/0975-7406.76462
[27] Losada-Pérez P, Mertens N, De Medio-Vasconcelos B, Slenders E, Leys J, Peeters M, et al. Phase transitions of binary lipid mixtures: a combined study by adiabatic scanning calorimetry and quartz crystal microbalance with dissipation monitoring. Adv Condens Matter Phys. 2015;14:479318.
[28] Diaz-Rohrer BB, Levental KR, Simons K, Levental I. Membrane raft association is a determinant of plasma membrane localization. Proc Natl Acad Sci. 2014 Jun 10;111(23):8500–5.